The Plant Cell, Vol. 13, 1263–1279, June 2001, www.plantcell.org

RESEARCH ARTICLE

The Arabidopsis *SERRATE* Gene Encodes a Zinc-Finger Protein Required for Normal Shoot Development

Michael J. Prigge[1] and D. Ry Wagner[2,3]

Institute of Molecular Biology, University of Oregon, Eugene, OR 97403

Organogenesis in plants depends upon the proper regulation of many genes, but how such necessary changes in gene expression are coordinated is largely unknown. The *serrate* (*se*) mutant of Arabidopsis displays defects in the initiation and elaboration of cotyledons and post-embryonic lateral organs. Cloning the *SE* gene revealed that it encodes a protein with a single, C_2H_2-type, zinc finger related to genes in other eukaryotes. Consistent with a role in organogenesis, the *SE* gene is transcribed in shoot meristems and in emerging organ primordia throughout development. Expression of the *SE* cDNA under the control of a heterologous promoter caused both accelerated and arrested plant growth, and these phenotypes were due to overexpression and co-suppression of the *SE* gene, respectively. Our analysis of the *se* mutant and the *SE* gene suggests a role for the *SE* gene product in regulating changes in gene expression via chromatin modification. Consistent with this proposed function, a synergistic double mutant phenotype was seen for plants mutant at both the *SE* locus and the locus encoding the largest subunit of chromatin assembly factor I.

INTRODUCTION

The aerial structures of a plant are produced by the shoot apical meristem, a collection of undifferentiated cells at growing shoot tips. Marked by drastically different rates of cell division, two zones within meristems can be distinguished (Steeves and Sussex, 1989). Slow cell divisions in the central zone serve to maintain this zone and to produce daughter cells for the peripheral zone. Cells in the peripheral zone rapidly proliferate to form organ primordia. Initiated reiteratively throughout plant development, organ primordia assume diverse fates depending on when and where they are initiated. Primordia initiated during the vegetative phase of development become leaves, while later primordia develop as floral meristems, which in turn produce sepal, petal, stamen, and carpel primordia. Furthermore, mature leaf structure differs depending on the developmental phase of the plant at the time of leaf initiation (Kerstetter and Poethig, 1998).

Along a cell lineage path from the central zone to the organ primordia, critical changes in gene expression occur. *Knotted1*-like homeobox (*knox*) genes are expressed throughout the meristem and downregulated in organ primordia (Reiser et al., 2000). Genes that are upregulated during organogenesis include the Arabidopsis *AINTEGUMENTA*, *PINHEAD/ZWILLE*, and *ASYMMETRIC LEAVES1* (*AS1*) genes (Elliott et al., 1996; Klucher et al., 1996; Lynn et al., 1999; Byrne et al., 2000), the snapdragon *PHANTASTICA* (*PHAN*) gene (Waites et al., 1998), and the maize *rough sheath2* (*rs2*) gene (Timmermans et al., 1999; Tsiantis et al., 1999). The *AS1*, *PHAN*, and *rs2* genes encode highly similar MYB-like proteins and are required for maintaining *knox* gene repression in developing leaves (Waites et al., 1998; Timmermans et al., 1999; Tsiantis et al., 1999; Byrne et al., 2000; Ori et al., 2000).

Given the sequential mechanism of organogenesis, genes that regulate widespread changes in gene expression are likely to be identified by mutations with pleiotropic effects on shoot and organ morphology. Here, we report the characterization of the Arabidopsis *SERRATE* (*SE*) gene. The *se* mutation has recently been shown to truncate the juvenile phase of vegetative development (Clarke et al., 1999; Serrano-Cartagena et al., 1999), increase plastochron lengths (Groot and Meicenheimer, 2000b), slow an early phase of leaf development (Groot and Meicenheimer, 2000a), and interact with *as1* and *as2* mutations with respect to *knox* gene repression in leaves (Ori et al., 2000). Our analyses of the *se* mutation revealed a pleiotropic phenotype affecting the positioning and the elaboration of leaves and floral organs. In

[1] Current address: Department of Molecular, Cellular, and Developmental Biology, University of Michigan, Ann Arbor, MI 48109-1048.
[2] Current address: Exelixis Plant Sciences, Inc., 16160 SW Upper Boones Ferry Road, Portland, Oregon, 97224. Telephone: 503-670-7702.
[3] To whom correspondence should be addressed. E-mail: rwagner@exelixis.com; fax 503-670-7703.

addition, the *se* mutation affects cotyledon initiation in embryos when the maternal parent is homozygous for the mutation. *SE* encodes a zinc-finger protein whose mRNA accumulates in meristems and organ primordia. Transgenic plants expressing the *SE* cDNA with a heterologous promoter displayed a range of phenotypes consistent with a role for the *SE* gene in organogenesis but not with a direct role in the regulation of vegetative phase transitions. These results indicate that the *SE* gene product plays a role in coordinating gene expression in the meristem and lateral organ primordia, possibly by regulating chromatin structure.

RESULTS

Phenotypic Characterization of the *se* Mutant

The *se* mutation was first utilized as a genetic marker for linkage map construction (Rédei and Hirono, 1964). The *se* mutation segregates as a single, recessive Mendelian trait albeit at a slightly reduced transmission rate (Table 1). The reduced transmission is likely due to lethality of *se/se* embryos rather than poor transmission through either gametophyte because similar allele transmission frequencies were observed for both heterozygous parents in test crosses (Table 1). Complementation tests indicated that *se* is not allelic to other serrated leaf mutants—*fas1*, *fas2*, *tousled*, and *leunig* (data not shown; Leyser and Furner, 1992; Roe et al., 1993; Liu and Meyerowitz, 1995); nor is it allelic to mutants that have been mapped to a similar position on chromosome II—*stunted plant1* and *emb152* (data not shown; Baskin et al., 1995; Vernon and Meinke, 1995). Every mutation conferring *se*-like phenotypes that arose in mutagenized populations screened in our laboratory complemented the *se* mutation (unpublished observations), and mutant screens performed by two other laboratories also failed to identify alleles (Berná et al., 1999; Clarke et al., 1999). Finally, a directed approach failed to identify new *se* alleles. Approximately 9000 progeny were generated by pollinating *se male* *sterile1-1* pistils with gamma- or UV-irradiated pollen from the Landsberg *erecta* (L*er*-0) ecotype. (The *male sterile1-1* mutation was included to prevent self-fertilization [van der Veen and Wirtz, 1968].) No progeny had a *se*-like phenotype and was heterozygous for L*er* flanking sequences (data not shown). These results show that the *se* mutation identifies a novel locus and may represent a unique lesion.

All leaf margins of the *se* mutant are serrated as compared with wild-type plants in which only leaves produced late in development are serrated (Figures 1A and 1B). In addition, mutant leaf margins—like those of later-produced wild-type leaves—do not curl abaxially (downward). Further analysis revealed a complex mutant phenotype that extends beyond leaf margin development.

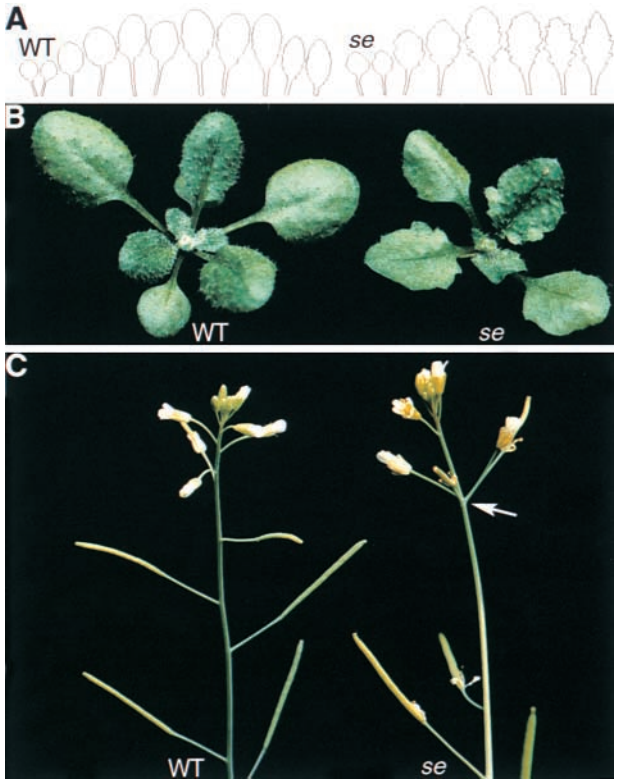

Figure 1. Phenotype of *se* Plants.

(A) Outlines of all the rosette leaves of a Columbia ecotype (Col-1; wild type) plant (left) and a *se* mutant plant (right). Rosettes of *se* mutant plants contain fewer leaves and all the leaves are serrated, whereas only later-produced leaves of Col-1 plants are serrated.
(B) Rosette of a Col-1 (wild type) plant (left) and a *se* mutant plant (right).
(C) Inflorescences of a Col-1 (wild type) plant (left) and a *se* mutant plant (right). The arrow points to an abnormal cluster of flowers and siliques on the *se* mutant inflorescence.
WT, wild type.

Table 1. Frequencies of Serrate Phenotype in Populations Segregating the *se* Mutation

Cross (Female × Male)	Serrate^{-}[a]	Wild Type[a]	Frequency[b] (%)	χ^2	P[c]
se/SE × *se/SE*	277	948	22.6	3.72	0.05
se/se × *se/SE*	419	495	45.8	6.32	0.01
se/SE × *se/se*	407	504	44.7	10.3	0.001

[a] The phenotypes of progeny from the given crosses were scored after the expansion of the first two true leaves.
[b] Percentage of progeny with a Serrate^{-} phenotype.
[c] The transmission frequency from each cross differed significantly from the expected Mendelian frequency ($P \leq 0.05$).

Several *se* mutant phenotypes reflect defects in the initiation and elaboration of lateral organs. Normally, lateral structures such as leaves and flowers are produced in a spiral arrangement, or phyllotaxy, with nearly constant radial and vertical displacement between adjacent appendages (Leyser and Furner, 1992). Rosettes and inflorescences of *se* mutant plants often exhibit significant deviations from the normal radial positioning, and the internode lengths between adjacent flowers were more random in *se* relative to wild-type plants (Figure 1C; data not shown). The *se* mutation exerts a subtle effect on flower development—extra sepals and petals and fewer stamens were frequently present in the earliest formed flowers (Table 2). Throughout vegetative development, mutant plants produced visible leaves at a rate ~70% of that observed for wild-type plants in the same growth conditions (Figure 2). This delay in leaf appearance may reflect a slower rate of leaf initiation or leaf elaboration, but two inflorescence phenotypes suggest that organ elaboration is primarily affected. First, because immature primordia in the shoot apex at the time of floral induction develop as either cauline leaves or as flowers, depending upon their developmental state (Hempel and Feldman, 1994), the increased number of cauline leaves on *se* mutant plants (Table 3) indicates that there are more immature leaf primordia at the time of floral induction. Second, *se* mutant inflorescences have an increased number of immature floral buds compared with those of wild-type inflorescences (Table 3), suggesting a slower rate of flower maturation.

In wild-type plants, the distribution of trichomes is developmentally regulated (Martínez-Zapater et al., 1995; Chien and Sussex, 1996; Telfer et al., 1997). Juvenile leaves produce trichomes only on the adaxial (upper) surface, whereas adult leaves produce trichomes on both the adaxial and abaxial surfaces. Under our growth conditions, wild-type plants generally produced six leaves lacking abaxial trichomes; however, *se* mutant plants produced only one or two leaves without abaxial trichomes (Table 3 and Figure 2). Furthermore, the first leaves bearing abaxial trichomes were visible nearly 5 days earlier on mutant plants than on wild-type plants, suggesting a defect in the regulation of this developmental phase transition (Figure 2). In addition to leaf margin serration and trichome distribution, other characteristics such as leaf shape and the number of hydathodes differ between early and late leaves and were similarly affected by the *se* mutation (Clarke et al., 1999; data not shown).

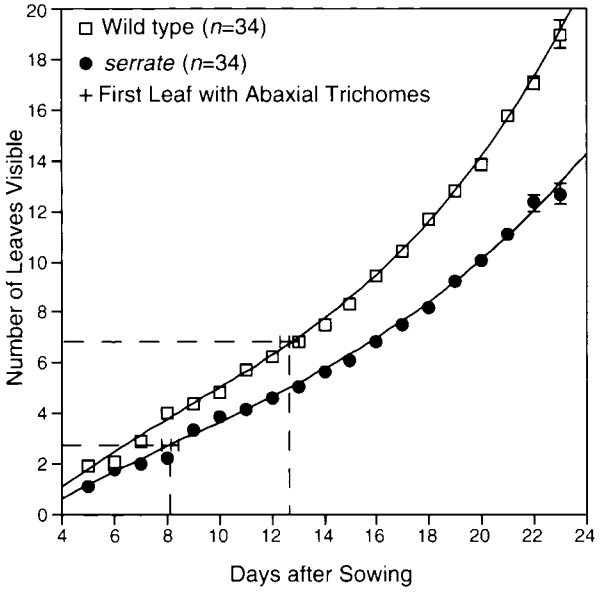

Figure 2. The *se* Mutation Affects the Rate of Leaf Production.

The number of leaves visible with the aid of a dissecting microscope were recorded daily, and the mean leaf number was plotted relative to the number of days since sowing. Error bars indicate ± twice the standard error. Col-1 (wild type) data points are indicated with open boxes, and *se* data points are indicated with filled circles. Superimposed onto this graph are the average leaf positions of the first adult leaves plotted against the average day on which these leaves were first visible.

Table 2. Numbers of Floral Organs in Wild-Type and *se* Mutant Basal Flowers

	Wild Type (Col-1)		*serrate*	
Whorl	Average[a]	Abnormal[b] (%)	Average[a]	Abnormal[b] (%)
Sepal	4.0 ± 0.0	0	4.3 ± 0.5	30
Petal	4.0 ± 0.0	0	4.3 ± 0.4	23
Stamen	5.5 ± 0.6	3	4.9 ± 0.8	37
Carpel	2.0 ± 0.0	0	2.0 ± 0.0	0
All whorls	15.5 ± 0.6	3	15.5 ± 1.0	63

[a] The number of floral organs in the first flower produced on 30 plants of both genotypes were counted and reported as the average ± twice the standard error.

[b] The percentage of deviation from the normal number of organs, which were four sepals, four petals, five or six stamens, and two carpels.

The *SE* gene is maternally required for normal embryo development. Whereas wild-type Arabidopsis embryos produced two cotyledons, progeny of selfed *se* plants often had either a single fused cotyledon or extra cotyledons (Figure 3). After reciprocal crosses using *SE*/*SE* or *se*/*SE* and *se*/*se* plants as parents, progeny cotyledon numbers were abnormal only when *se*/*se* plants were used as the maternal parent (Figure 3). These data indicate that the *se* mutation exerts its effect on embryo patterning from the surrounding maternal tissue and not from the gametophyte, endosperm, or embryonic cells. Consistent with this, seven out of thirteen aberrant progeny from the cross involving *se*/*se* (maternal parent) and *se*/*SE* (pollen donor) were genotypically heterozygous at the *SE* locus and displayed otherwise normal post-embryonic development (data not shown).

Table 3. Developmental Phase Transitions in Wild-Type and *se* Mutant Plants

	Number of Leaves[a]				
Genotype	Juvenile	Adult	Cauline	Flowering Time[b]	Flower Buds[c]
Wild type (Col-1)	5.8 ± 0.4	10.1 ± 0.6	3.9 ± 0.3	22.4 ± 0.5	16.9 ± 1.1
serrate	1.8 ± 0.3	8.4 ± 0.8	5.2 ± 0.6	22.6 ± 1.0	26.8 ± 2.6

[a] Adult rosette leaves were defined as those with trichomes on the abaxial leaf surface, whereas juvenile rosette leaves lacked abaxial trichomes. Only cauline leaves on primary inflorescence were included; $n = 30$; mean ± twice the standard error.

[b] Days until flower buds were visible; $n = 30$; mean ± twice the standard error.

[c] When the primary inflorescences had between 10 and 25 post-anthesis flowers, the number of developing flower buds (between stages 6 and 12) were counted; mean ± twice the standard error. Wild type, $n = 35$; serrate, $n = 25$.

Similar to the rate of leaf production, the rate of root growth was also slower in *se* mutants. When the changes in primary root length during day 7 of growth were compared, *se* roots elongated at a rate ~70% of that observed in wild-type roots (*se*, 5.5 ± 0.4 mm; wild type, 8.2 ± 0.7 mm; mean ± twice the standard error).

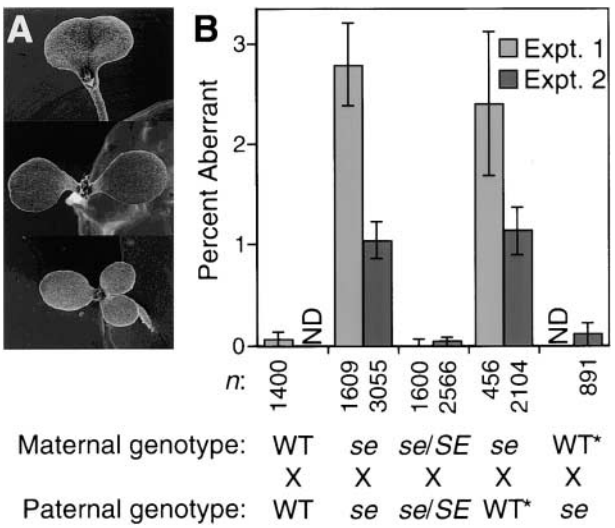

Figure 3. Maternal Effects of the *se* Mutation.

(A) Variation in cotyledon number in week-old progeny from *se* mutant ovules.

(B) After germination, the number of seedlings with abnormal cotyledon numbers were counted. Error bars indicate ±SD of the binomial distribution. Experiments (Expt.) 1 and 2 differ only in the growth conditions of the parents: Experiment 2 was performed in a greenhouse during the winter. Supplemented artificial light was provided from 8:00 A.M. to midnight, and the daytime temperatures were held at less than ~25°C (nighttime temperatures were cooler). Asterisks denote that wild-type (Col-1) plants were used in this cross for experiment 1 and *se/SE* plants in experiment 2. *n*, total number of seedlings scored; ND, not determined.

The *SE* Locus Encodes a Zinc-Finger Protein

The complex *se* mutant phenotype suggests that the *SE* gene product regulates the activity of a number of developmental pathways. To help decipher its role in development, we isolated the *SE* gene by positional cloning (Figure 4). Genetic linkage to the middle of chromosome 2 had previously been reported (Rédei and Hirono, 1964), and this was confirmed using the *GPA1* cleaved amplified polymorphic sequence (CAPS) marker (Konieczny and Ausubel, 1993). Using mapping lines with meiotic recombination breakpoints near the *SE* locus, *SE* was determined to be between the *GPA1* and the nga1126 (http://thale.salk.edu/) loci. A bacterial artificial chromosome (BAC) contig was assembled extending from the *GPA1* locus. During contig assembly, restriction fragment length polymorphism (RFLP) markers derived from BAC end sequences were mapped relative to *SE* until it was found that the T6E21-Sp6 RFLP marker mapped distally from the *SE* locus. BAC T9H20 spanned most of the region between flanking RFLP markers genetically separable from *SE* and was subcloned for plant transformation. Of 13 cosmids introduced into *se* mutant plants, four conferred a wild-type phenotype. Within the 10-kb region shared by the complementing cosmids, a single complete gene and two partial genes were found by DNA sequence analysis. Flanking cosmids that deleted portions of the complete gene but spanned either of the partial genes did not rescue the mutant phenotype. Furthermore, the complete gene contained a 7-bp deletion in the corresponding region from the *se* mutant genome, confirming that this was the *SE* gene.

The *SE* open reading frame encodes a 720–amino acid protein predicted to contain a single C_2H_2-type zinc finger and multiple bipartite nuclear localization motifs (Figure 5A). The *se* mutation would cause a frameshift altering the last 27 amino acids. Two expressed sequence tags (ESTs) from sugarcane that were highly similar to the C terminus of the predicted SE protein were present in public databases and were used to isolate two distinct *SE* homologs from another monocot, maize. The amino acid sequences encoded by

three partial monocot cDNAs (from sugarcane and maize) share ~90% identity with one another and 60% identity with the dicot-derived SE protein. Currently, the public databases contain homologous ESTs from maize (six accessions), rice (two), sorghum (eleven), tomato (three), potato (one), soybean (one), and hybrid aspen (one). In addition, several genomic survey sequences (four BAC end sequences and the RG365 RFLP marker sequences) from rice contain sequence similarity to the *SE* gene. The maize genome contains at least four *SE*-related genes because the ESTs identify genes distinct from those isolated using the sugarcane cDNA sequence (Figure 5A). The rice and sorghum genomes, however, appear to have only two expressed *SE*-related genes. An alignment of SE-related sequences from plants is shown in Figure 5A.

Significant homology is also shared with the SPBC725.08 zinc-finger protein of unknown function from *Schizosaccharomyces pombe* and a protein family from animals that includes the hamster arsenite resistance2 (Asr2) protein (Rossman and Wang, 1999). Although the overall similarity between the plant, fungal, and animal proteins is modest (11 to 15% amino-acid identity), the sequences and relative orders of four domains are conserved (Figure 5B). Significantly, two of these domains correspond to the zinc-finger domain and the C-terminal sequences affected by the *se* mutation. Interestingly, the animal homologs lack the second conserved cysteine but retain high similarity in the region corresponding to the DNA binding helix of other zinc fingers (Figure 5B; Klug and Schwabe, 1995; Berg and Shi, 1996). Although no biochemical function has been ascribed to any of these proteins, overexpression of the *asr2* cDNA—which is likely to encode only a portion of the full-length protein—confers arsenite resistance to hamster cell lines (Rossman and Wang, 1999).

Expression Pattern of the *SE* mRNA

The *se* mutant phenotype suggested that the wild-type *SE* gene product is required for normal development of shoot and floral meristems, developing leaves, and embryos. *SE* mRNA was detected in all of these tissue types by use of in situ hybridization (Figure 6; data not shown). In the developing embryo, *SE* expression is present in the shoot and root meristems and in the adaxial portion of cotyledons of torpedo-stage embryos, but expression is reduced in walking-stick stage embryos and absent from mature embryos (Figures 6A to 6C). Similar to cotyledons, the adaxial portion of newly emerging leaf primordia exhibits the highest level of *SE* expression, but more mature leaves retain some expression only in localized regions (Figure 6E). The downregulation of *SE* is rapid during floral organ development: for example, *SE* mRNA is detected in sepal primordia of stage 4 flowers, but by stage 7, expression is absent from sepals and is present in the emerging stamen and carpel primordia

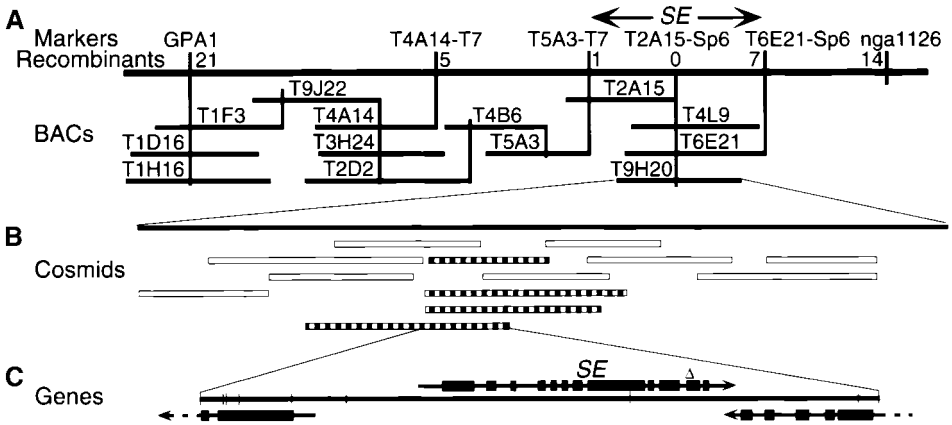

Figure 4. Positional Isolation of the *SE* Locus.

(A) Position of *SE* relative to polymorphic markers in the middle of chromosome 2 (long, thick horizontal line) and the contig of BACs (horizontal bars). The vertical lines represent the positions of DNA fragments used for mapping (those named across the top) or those used only for constructing the BAC contig (unnamed). The number of meiotic recombination events identified between a marker and the *se* mutation are indicated below the marker names.

(B) Cosmid subclones of the BAC T9H20 (solid bar). Striped bars indicate cosmid subclones that complemented the *se* mutant phenotype upon transformation, and open bars indicate those that did not.

(C) Schematic representation of the gene structures in the region that complemented the *se* mutant phenotype. Filled boxes represent exons, lines designate noncoding regions, arrowheads show the direction of transcription, and dashed lines indicate that the genes extend beyond the region sequenced. The position of the 7-bp deletion of the *se* mutant genome is indicated (open triangle).

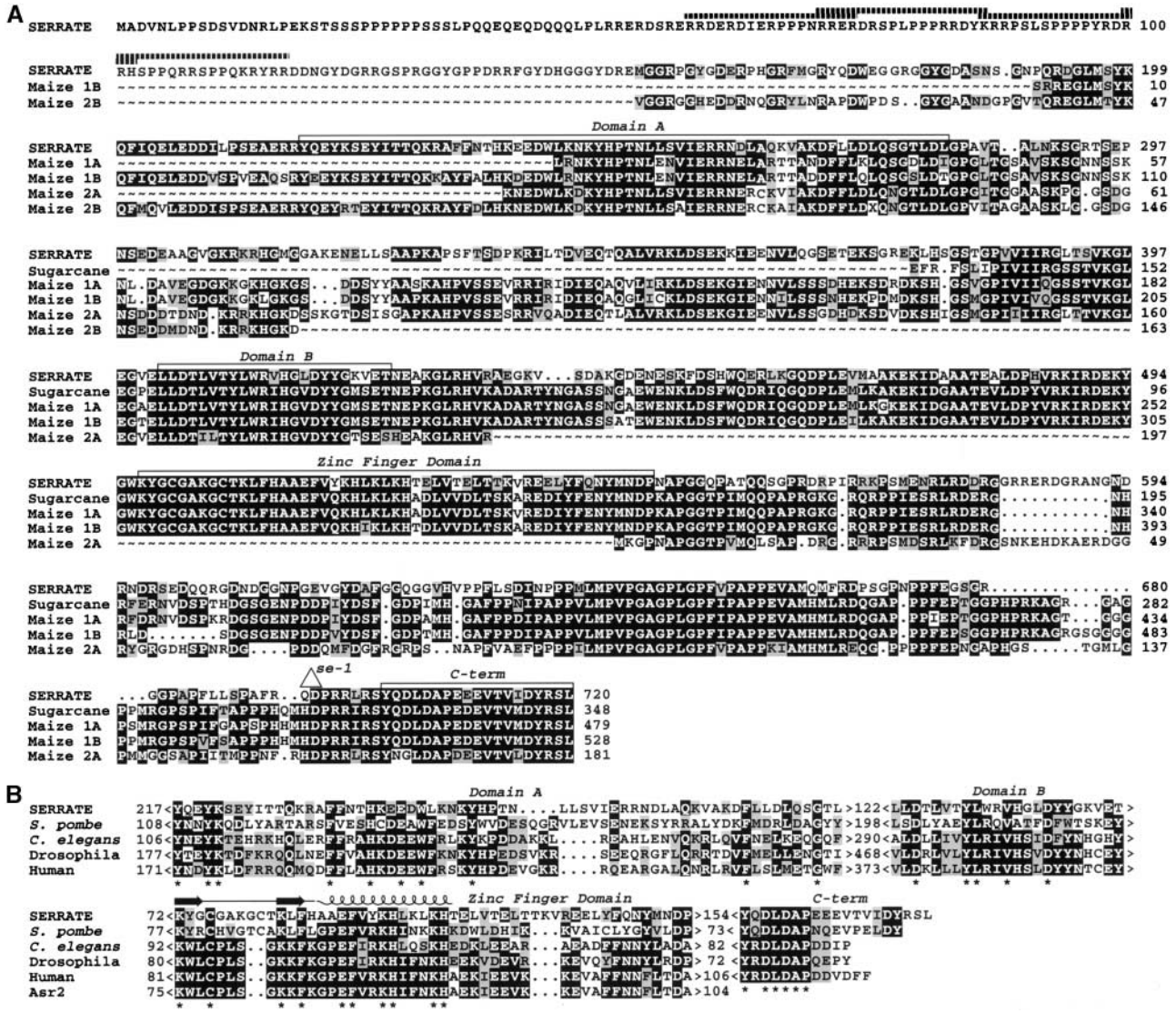

Figure 5. SE Is a Member of a Protein Family Conserved in Eukaryotes.

(A) Alignment of SE-related sequences from plants. Conserved residues are shaded in black, and conservative changes are shaded in gray. Gaps (indicated by dots) were introduced to optimize alignment, and tildes (~) were added where sequence information is lacking. The sources of the sequences are described in Methods. The positions of the four domains used in the alignment shown in **(B)** are designated with brackets and labeled, and the positions of *se-1* mutation and putative bipartite nuclear localization motifs are indicated with a triangle and hatched bars, respectively. Genes designated ZmSExx are derived from maize. C-term, C terminus.

(B) Alignments of four domains (A, B, zinc finger, and C terminus) of the predicted SE protein with comparable domains of the *S. pombe* SPBC725.08 protein; the Asr2-related homologs from *Caenorhabditis elegans*, Drosophila, and human; and the Chinese hamster Asr2 protein. Shading is as described for **(A)**, and residues conserved in all homologs are highlighted with an asterisk. The number of residues in front of and between domains are indicated. The positions comparable to the two β strands and the α helix of C_2H_2-zinc-finger domains of known structure are indicated with arrows and a coil above the respective sequences.

(Figure 6F; stages as defined in Smyth et al., 1990). *SE* mRNA is also detected throughout vegetative, inflorescence, and floral meristems (Figures 6E and 6F). *SE* mRNA accumulation in *se* mutant apices appears to be reduced in parallel in situ hybridization experiments, suggesting either that the C-terminal sequences may be required for autoregulation or that the small deletion adversely affects mRNA stability (Figure 6G).

Phenotypic Effects of *SE* Misexpression

The *SE* locus was identified based upon a single mutation affecting only the C-terminal tail of the predicted protein. To observe the effects of altered levels of *SE* activity, wild-type and *se* mutant plants were transformed with the *SE* cDNA under the control of the cauliflower mosaic virus 35S RNA (35S) promoter (Odell et al., 1985). A range of phenotypes arose in the T_1 plants, but a significant proportion of these lines (29/67) could not be recovered due to seedling lethality or sterility. The phenotypes of the T_2 generation were studied in greater detail, and two classes emerged (Table 4, and Figures 7A and 7B). Class I lines displayed an essentially wild-type phenotype whether in a wild-type or *se* mutant background, and class II lines displayed a range of developmental phenotypes. Interestingly, lines carrying the *se* mutation tended to have more severe phenotypes than did those transformed into a wild-type background (Table 4). Furthermore, the severity of the class II lines frequently increased with successive generations regardless of the background. For example, the sbla3 T_1 plant (in *se* background) was fertile, but every T_2 plant was completely sterile ($n > 20$). Given the phenotypic instability of class II lines, and the class I and class II phenotypes (below), class I lines are likely to be overexpressing the *SE* gene and class II lines are likely to have suppressed *SE* function.

One class I line in the *se* mutant background, sbla11, was chosen for detailed analysis because the transgene stably complemented all of the *se* mutant phenotypes (Figure 7A and Table 5) and exhibited high levels of *SE* mRNA expression (Figure 7I). In contrast to the *se* mutant, the sbla11 plant line displayed an increased rate of leaf production and had a decreased number of developing floral buds on inflorescences relative to wild-type plants (Table 5). Unexpectedly, the transgene also affected both the number of days and the number of leaves produced prior to flowering (Table 5). Each vegetative phase is shortened relative to those of wild-type plants, suggesting that development in general is accelerated by *SE* overexpression.

Class II lines displayed strikingly variable phenotypes both within and between lines. The class was further subdivided based upon the more severe phenotypes appearing in T_2 families (Figure 7B). Mildly affected (class IIa) lines produced relatively normal leaves but consistently developed inflorescence phyllotaxy defects similar to those seen in *se* mutants. The intermediate class of transformants (class IIb) produced leaves with adaxially curled lamina and reduced inflorescence internode elongation. Growth of the severely affected (class IIc) lines intermittently arrested after the production of a variable number of leaves (most often after 0, one, or two leaves; Figure 7D). Microscopic analysis of arrested shoot apices revealed protrusions with outgrowths emerging along their sides (Figure 7E). On the basis of their positions and morphology, the tips of these protrusions are likely to be apical meristems, and the outgrowths appear to be arrested organ primordia. Eventually, growth continued, with new leaf primordia emerging both from the original meristem's location and from positions on the side of the apex. The leaves produced by class IIc lines were similar to those of the *se* mutant but were often asymmetric in shape (data not shown). The inflorescences of these plants were severely affected: there was little internode elongation between cauline leaves, and few flowers were produced (Figure 7F; data not shown). The flowers that did form were disorganized and had extremely variable numbers of floral organs and radially symmetric filaments (Figures 7F to 7H). In several class IIc lines, floral meristems failed to terminate properly after the production of the carpel whorl, resulting in sterile masses predominately composed of unfused carpels and exposed ovules (Figure 7H).

The range of phenotypes seen in the 35S::*SE* transformants suggested that expression from the transgene might be variable. After the T_1 plants were phenotypically scored, gene expression was analyzed by semi-quantitative reverse transcriptase–polymerase chain reaction (RT-PCR). As shown in Figure 7I, expression levels were variable, but there was only a slight correlation between phenotypic class and *SE* mRNA accumulation. This poor correlation suggests either that a post-transcriptional mechanism is responsible for the phenotypic variability or that transcript accumulation is spatially and/or temporally variable and was not adequately assayed by our analysis of mature leaf tissue.

Synergistic *se fas1* Double Mutant Phenotype

Mutations in the *FAS1* gene cause pleiotropic phenotypes that overlap the phenotypes observed for *se* mutants: mutations in either gene affect leaf serration, phyllotaxy, and the numbers of floral organs in the outer three whorls (Figure 8A; Leyser and Furner, 1992). Unlike *se*, however, *fas1* mutants have narrow leaves and enlarged meristems that often lead to stem fasciation. To determine whether the *SE* and *FAS1* genes function in a common pathway or in converging pathways, double mutants were constructed. Two *fas1* alleles from the En ecotype background were used in these analyses. The inflorescence phenotypes are similar, but the *fas1-11* allele caused more deeply serrated leaves and less fertile flowers than did the *fas1-1* mutant allele (Serrano-Cartagena et al., 1999; data not shown). Despite having a less severe phenotype, molecular analysis suggests that *fas1-1* is a null allele (Kaya et al., 2001). The *se fas1-1* and *se*

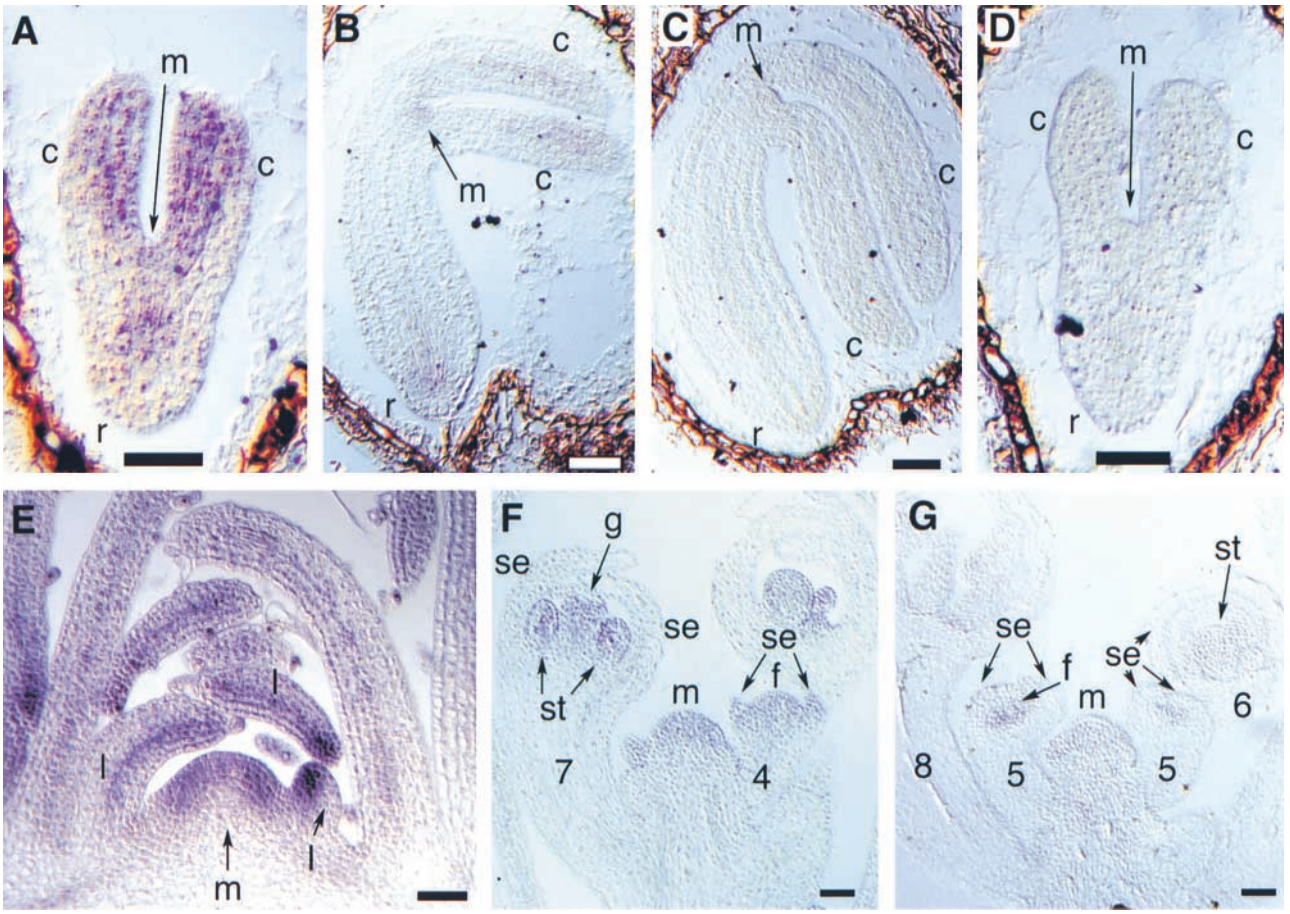

Figure 6. In Situ Localization of *SE* mRNA in Wild-Type and *se* Mutant Tissue.

(A) to **(C)** Torpedo-stage **(A)**, walking-stick stage **(B)**, and nearly mature **(C)** wild-type embryos hybridized with an antisense *SE* riboprobe.
(D) Torpedo stage wild-type embryo hybridized with a sense (control) *SE* riboprobe.
(E) Apex of the wild-type shoot apex prior to flower production but after hybridization with an antisense *SE* riboprobe.
(F) and **(G)** Wild-type **(F)** and *se* mutant **(G)** inflorescences hybridized with an antisense *SE* riboprobe. Numbers indicate stage of flower development.
c, cotyledon; f, floral meristem; g, developing gynoecium; l, leaf primordia; m, shoot apical meristem; r, root meristem; se, developing sepal; sf, developing stamen. Bars = 40 μm.

fas1-11 double mutants produced a variable number of extremely narrow lateral organs before the meristems degenerate into masses of callous-like cells (Figures 8B to 8E). Out of 59 *se fas1-1* double mutants, 42 (71%) arrested prior to stem elongation, seven (12%) arrested after inflorescence elongation but prior to flower formation, and 10 (17%) arrested only after the initiation of a few misshapen flowers (Figure 8B). The last leaves produced prior to meristem degeneration often had radial symmetry (data not shown). Similar phenotypes were previously reported for the *mgo1-1 fas1-1* double mutant (Laufs et al., 1998). This synergistic genetic interaction suggests that the *SE* and *FAS1* genes function in separate pathways that converge during organogenesis, but a common-pathway model cannot be completely dismissed because the *se* mutation is not likely null.

DISCUSSION

The phenotypes of the *se* mutant indicate a role for the SE protein in organogenesis. The slower rate of leaf production, the displacement of more leaves onto the inflorescence stem, and the presence of more immature flower buds are all consistent with a primary defect in the early steps of organ elaboration. This interpretation is also consistent with

the analyses by Groot and Meicenheimer (2000a) that revealed that growth of *se* leaves is biphasic, with slower growth early (until ~2 mm in length) and normal growth thereafter. Detailed mutational analysis of the *SE* gene was handicapped by the lack of additional mutant alleles. Allelic mutants have not been identified based on leaf phenotypes in our laboratory or in screens by other laboratories (data not shown; Berná et al., 1999; Serrano-Cartagena et al., 1999; Clarke et al., 1999). Furthermore, a directed pollen-mutagenesis approach also failed to identify new alleles. One explanation for the failure to identify new alleles is that the original *se* allele retains some function that is essential for development. This is consistent with molecular analysis of the existing *se-1* mutant allele, which only affects the C-terminal 27 amino acids (Figures 5A). Despite the uniqueness of the *se-1* allele, it is unlikely that the phenotype results from the gain of a novel function because the mutation acts recessively.

Analysis of transgenic plants misexpressing the *SE* gene revealed two classes of phenotypes. The nearly wild-type phenotype of class I lines suggests that SE activity is permissive for normal development because ectopic *SE* expression rescues the mutant phenotypes with few additional consequences. These lines produce leaves at a slightly faster rate than do wild-type plants, but the most profound effect was on flowering time, suggesting that the SE protein may be involved in the vegetative-to-floral phase transition as well as the transitions from meristematic to organogenetic growth. Given the appearance of phenotypes similar to those found in the *se* mutant, class II lines appear to have reduced *SE* function due to co-suppression (Matzke and Matzke, 1998). Although the increase in phenotypic severity in several of the class II lines in successive generations suggests an epigenetic mechanism, there was little correlation between phenotypic severity and transgene mRNA expression (Figure 7I). One explanation for this is that the *SE* gene is essential and that stably silenced plant lines were lost due to selection of viable transformants. In this scenario, *SE* expression in the class II lines is unstable and therefore detectable in total leaf RNA preparations. Alternatively, SE function may be suppressed by a "squelching" mechanism. Genetic squelching may result when a protein is overexpressed and dilutes the pool of required co-factors (Ptashne, 1992; Larkin et al., 1994).

The relationship of the organ elaboration phenotypes with the leaf margin and the trichome distribution phenotypes is unclear. One possibility—corroborated by *SE* mRNA expression pattern (Figure 6) and the *SE* misexpression phenotypes (Figure 7)—is that there is an associated defect in leaf polarity in lateral organs of the *se* mutant. Organogenesis and organ polarity defects are linked in other mutants. The *phan* mutants of snapdragon fail to initiate organ primordia at low temperatures and produce partially or completely abaxialized organs at higher temperatures (Waites and Hudson, 1995; Waites et al., 1998). Strong mutant alleles of the Arabidopsis *ARGONAUTE1* (*AGO1*) gene produce organs at a much slower rate than do wild-type plants, and many organ types are abaxialized in the mutant (Bohmert et al., 1998; Lynn et al., 1999). Weaker *ago1* mutants display a delay in organ production and allele-specific defects in organ patterning: one class of alleles produces narrow organs and another class produces serrated leaves that are frequently trumpet shaped and have outgrowths on the abaxial surfaces—both likely due to a partial adaxialization of organ primordia (Champagne, 1998). Although trumpet-shaped leaves have never been observed in *se* mutants, the phenotypes of the latter class of weak *ago1* mutants and the *se* mutant are remarkably similar and suggest that *SE* and *AGO1* act in overlapping developmental pathways. Both mutants display slow rates of organ production, similar leaf margin morphologies, and flower-positioning defects.

The embryo's dependence on *SE* activity for proper cotyledon initiation is interesting, and similar maternal control over plant embryo patterning has only previously been observed for the Arabidopsis *sin1-2* mutant and transgenic tobacco plants overexpressing the oat *phyA* gene (Ray et al., 1996; Emmler and Schäfer, 1997). Given the presence of a haploid gametophyte generation between diploid sporophyte generations, maternal effects on plant embryo development are paradoxical because the embryo is isolated both spatially (by the endosperm) and mitotically (during megagametophyte development) from diploid maternal tissue. One possibility is that the SE and SIN1 proteins may be involved in establishing the expression state of one or more maternal genes prior to gametogenesis. The *MEDEA*/*FIS1* gene of Arabidopsis is required for proper embryo and endosperm development and was recently found to be imprinted such that only maternally inherited copies are expressed during endosperm development (Chaudhury et al., 1997; Grossniklaus et al., 1998; Kinoshita et al., 1999; Kiyosue et al., 1999; Luo et al., 1999; Vielle-Calzada et al., 1999). In another possibility, the *SE* and *SIN1* genes may be involved in signaling to the early embryo positional information required for the proper induction of bilateral symmetry. A third

Table 4. Phenotypic Categories of 35S::*SE* Lines[a]

	Number of Independent Lines per Class (%)			
Background	Class I	Class IIa	Class IIb	Class IIc
serrate	3 (11%)	1 (4%)	10 (36%)	14 (50%)
Wild type (Col-1)	4 (36%)	3 (27%)	3 (27%)	1 (9%)

[a] The 35S::*SE* construct was transformed into *se* and wild-type plants, and the T_2 transgenic lines were grown for ~2 weeks before scoring the phenotypes. The phenotypes were classified based on the most severe segregants as described in the text: class I, wild type; IIa, mild; IIb, intermediate; and IIc, severe. The probability that the observed distribution of phenotypes was independent of genetic background was <0.02 using a 2×4 William's corrected *G* test of independence.

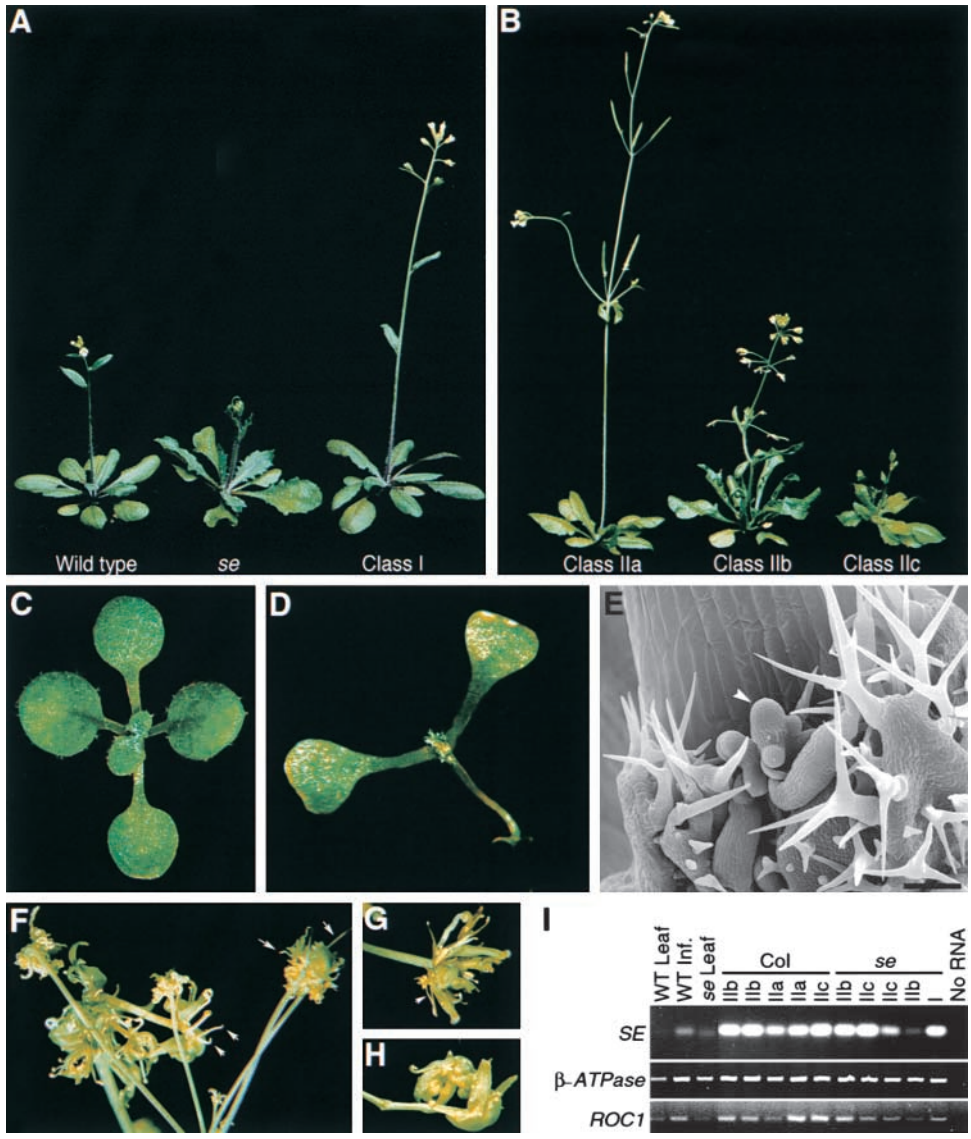

Figure 7. Phenotypes of Plants Harboring the 35S::*SE* Transgene.

(A) A class I (sbla11) T_4 plant is compared with the wild type (Col-1) and the *se* mutant after ~25 days of growth. The class I plant's inflorescence is taller due to the early flowering phenotype.

(B) The phenotypes of classes IIa (sbla6), IIb (sbla1), and IIc (sala3) T_3 plants are compared after ~30 days of growth. Note the aberrant flower positions of the classes IIa and IIb plants and the aberrant leaf positioning of the class IIc plant.

(C) Ten-day-old wild-type seedling with two cotyledons and four true leaves.

(D) Ten-day-old class IIc (sbla17) plant that arrested after cotyledon expansion.

(E) Scanning electron micrograph of an arrested apex of a class IIc line. The arrowhead points to the meristem, which is flanked by arrested primordia. Magnification bar is ~100 μm.

(F) to **(H)** Examples of the various inflorescence and flower patterning defects seen in class IIc lines. Note the wide range in floral organ numbers and organ morphologies. The mature "flower" shown in **(H)** failed to terminate after the production of carpels. Arrows point to radially symmetric filaments.

(I) Detection of *SE* mRNA in *SE* misexpression lines. Total leaf RNA was prepared from 10 T_1 plants of the given phenotypic class, and *SE* mRNA was detected by semi-quantitative RT-PCR. The lines represented include cbla1, cala2, cala3, cala4, and cala7 in a wild-type background, and sbla2, sbla3, sbla4, sbla10, and sbla11 in a *se* mutant background. For control reactions, cDNA was prepared from wild-type leaves (WT Leaf), wild-type inflorescences including pre-anthesis flower buds (WT Inf.), and *se* leaves (*se* Leaf). The gel at top shows the detection of *SE* mRNA, whereas the bottom two gels show detection of the ubiquitously expressed *β–ATPase* and *ROC1* genes (Boutry and Chua, 1985; Kelly et al., 1990; Lippuner et al. 1994). Note that the *SE* RT-PCR product from *SE* leaves is slightly smaller than that from the wild type due to the mutation.

Table 5. Phenotypic Analysis of the sbla11 Class I 35S::*SE* Line

	Number of Leaves Visible[a]			Number of Leaves[b]				
Genotype	Day 6	Day 11	Day 16	Juvenile	Adult	Cauline	Flowering Time[c]	Flower Buds[d]
35S::*SE se*	2.0 ± 0.0	5.8 ± 0.2[e]	11.6 ± 0.3[f]	4.2 ± 0.2[f]	5.8 ± 0.3[f]	2.7 ± 0.1[f]	18.6 ± 0.3[f]	15.1 ± 1.9[e]
Wild type (Col-1)	2.0 ± 0.1	5.5 ± 0.2	11.0 ± 0.3	4.6 ± 0.3	7.9 ± 0.4	3.7 ± 0.2	20.9 ± 0.4	17.0 ± 1.0
serrate	0.0 ± 0.0[f]	4.0 ± 0.1[f]	7.8 ± 0.2[f]	1.9 ± 0.2[f]	5.8 ± 0.4[f]	4.6 ± 0.4[f]	21.1 ± 0.5	30.7 ± 1.4[f]

[a] On given days after sowing, the number of leaves visible without dissection and using a dissecting microscope were recorded; mean ± twice the standard error; $n = 45$ to 48.

[b] Adult rosette leaves were defined as those with trichomes on the abaxial leaf surface, whereas juvenile rosette leaves did not have abaxial trichomes. Only cauline leaves on primary inflorescence were included. Mean ± twice the standard error; $n = 45$ to 48.

[c] Days until flower buds were visible; mean ± twice the standard error; $n = 45$ to 48.

[d] When the primary inflorescences had between 10 and 25 post-anthesis flowers, the number of developing flower buds (between stages 6 and 12) were counted; mean ± twice the standard error; $n = 25$ to 35.

[e] Significantly different from the wild type ($P < 0.05$).

[f] Significantly different from the wild type ($P \leq 0.001$).

possibility is that sufficient maternally contributed wild-type protein or mRNA persists through gametogenesis and early embryogenesis and that zygotic expression appears too late to rescue the defect in embryo symmetry.

The putative zinc-finger and nuclear localization motifs suggest that the SE protein regulates transcription, possibly by altering chromatin structure. Unlike conventional zinc-finger transcription factors (Klug and Schwabe, 1995; Berg and Shi, 1996), SE contains a single zinc finger—rather than tandem repeats—and is, consequently, unlikely to bind alone with high sequence specificity. Having lower levels of sequence specificity would allow SE to coordinate the expression of many genes by altering chromatin structure in a region-specific manner. Previous analyses of leaf-shape mutants have already established a link between gene silencing and leaf development. Mutations in the *CURLY LEAF* gene of Arabidopsis, encoding an E(z)-like polycomb-group protein, cause the leaf lamina to roll up as a result of ectopic expression of the floral homeotic gene *AGAMOUS* (Goodrich et al., 1997). The leaf curling phenotype of class IIb 35S::*SE* plants is very similar to that of *curly leaf* mutants, suggesting that SE might also be involved in repressing the *AGAMOUS* gene, and preliminary RT-PCR results agree with this interpretation (M.J. Prigge and D.R. Wagner, unpublished results).

A role for SE in gene regulation during organogenesis was recently identified by analysis of the *se as1* and *se as2* double mutants. The *se* mutation synergistically enhanced the *as1* and *as2* phenotypes, resulting in phenotypes very similar to those of plants overexpressing the *KNAT1 knox* gene—including the appearance of ectopic stipules in the sinuses of leaf lobes (Ori et al., 2000). Although *as1* and *as2* single mutants ectopically express the *KNAT1* and *KNAT2 knox* genes in leaf tissue, only rarely do ectopic stipules develop (Byrne et al., 2000; Ori et al., 2000). Although *se* single mutants do not express *knox* genes ectopically, *se as1* and *se as2* double mutants exhibit slightly increased *knox* gene expression in the sinuses but reduced expression in other parts of leaves relative to *as* single mutants (Ori et al., 2000). This suggests that the *se* mutation either allows *knox* gene expression to rise above a critical threshold specifically in leaf margins, lowers the *knox* gene expression threshold required to activate downstream genes, or a combination of both possibilities. A role for the SE protein in regulating chromatin structure would be consistent with both of these possibilities.

Two other proteins with single C_2H_2 zinc fingers have been implicated in regulating chromatin structure: FIS2 from Arabidopsis (Luo et al., 1999) and the GAGA factor (GAF) encoded by the *Trithorax*-like gene of Drosophila (Farkas et al., 1994; Pedone et al., 1996). Although no target genes have been identified, mutant analysis suggests that FIS2 is required for repressive chromatin structure during megagametophyte development in the same pathway as two polycomb-group genes: *FIS1*/*MEDEA* and *FIE*, which are homologous to the Drosophila E(z) and Esc proteins, respectively (Chaudhury et al., 1997; Grossniklaus et al., 1998; Kiyosue et al., 1999; Luo et al., 1999; Ohad et al., 1999). In contrast to the proposed role for FIS2, GAF antagonizes silent chromatin maintenance, resulting in timely derepression of several developmentally and environmentally regulated genes (reviewed in Wilkins and Lis, 1997). In a manner analogous to the FIS2 and GAF proteins, SE may coordinate the expression of multiple genes during development by modifying the chromatin structure surrounding these genes.

The synergistic genetic interaction between *se* and *fas1* mutations is most easily explained as a convergence of two pathways regulating chromatin structure. *FAS1* encodes the largest subunit of chromatin assembly factor I (Kaya et al., 2001), which directs assembly of histones onto newly replicated DNA (Smith and Stillman, 1989; Adams and Kamakaka, 1999). Mutations in the yeast homolog *CAC1*/

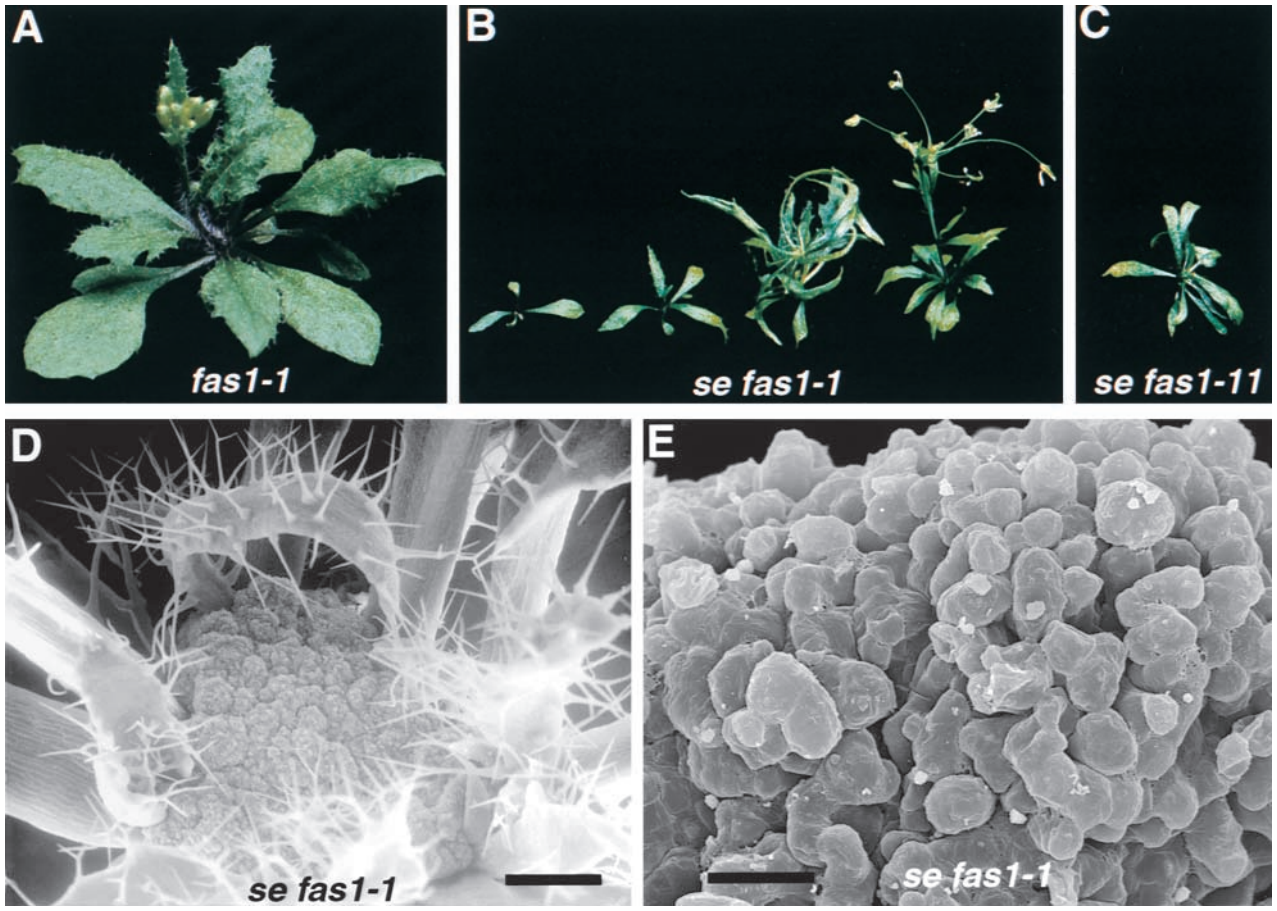

Figure 8. *se fas1* Double Mutant Phenotype.

(A) *fas1-1* single mutant.
(B) Range of phenotypes displayed by ~28-day-old *se fas1-1* double mutants. Note that all leaves are extremely narrow and that the shoot apex has arrested growth in each individual albeit at different developmental times.
(C) *se fas1-11* double mutant.
(D) and **(E)** Scanning electron micrographs of the arrested shoot apex of an ~30-day-old *se fas1-1* double mutant plant. The meristem has degenerated into a mass of callous-like tissue. Bar in **(D)** = ~500 μm; bar in **(E)** = 20 μm.

RLF2 impair the maintenance of gene silencing at the telomeres and at the silent mating loci (Enomoto et al., 1997; Kaufman et al., 1997; Enomoto and Berman, 1998). Reminiscent of the *fas1* interaction with *se*, *cac1/rlf2* mutants interact synergistically with mutations in the *SIR1* gene (Enomoto and Berman, 1998). Because SIR1p is required for the establishment of gene silencing at the silent mating loci (Pillus and Rine, 1989), it was proposed that SIR1p cooperates with chromatin properly assembled by CAC1/RLF2p function (Enomoto and Berman, 1998). An intriguing possibility is that SE protein may downregulate genes during organogenesis in a manner analogous to SIR1p.

In an alternative hypothesis, *SE* may be directly regulating the cell cycle. Such a hypothesis is consistent with the *SE* mRNA accumulation pattern (the highest expression in tissue with the shortest cell-cycle lengths) and with the *SE* overexpression phenotypes because similar phenotypes were seen when an Arabidopsis D-type cyclin was overexpressed in tobacco (Cockcroft et al., 2000). A role for *SE* in cell-cycle regulation is, however, less easily reconciled with the phenotype of the *se fas1* double mutant in which cell division continued after organogenesis had arrested (Figure 8D). Further investigations of the SE protein function should reveal the mechanism by which *SE* regulates so many aspects of plant development.

METHODS

Plant Materials, Culture, and Analysis

Arabidopsis thaliana seed for the *se*, *fas1-1*, *fas1-11*, and *phyB-10* mutant strains and the Columbia (Col-1) and Wassilewskija (Ws-2) wild-type strains were obtained from the Arabidopsis Biological Resource Center (ABRC, Ohio State University, Columbus). Eva Sundberg and George Coupland (John Innes Centre, Norwich, UK) supplied Tn28 and *alb3-1* seed (Long et al., 1993).

Seeds were imbibed at 4°C for 3 to 5 days before or after sowing to 6-cm square pots containing coarse vermiculite overlaid with a 1- to 2-cm layer of soil mix comprised of a 2:1 mixture of Premier Pro potting soil (Red Hill, PA) and fine vermiculite. Plants were grown either in a long-day growth room (18-hr-light:6-hr-dark cycle) or in a greenhouse during the winter with supplemented light. Temperatures in the growth room were maintained between 18 and 22°C, but the greenhouse temperatures were very variable with cooler nighttime temperatures. Peters Professional (20-20-20) fertilizer was administered upon sowing and again after ~3 weeks of growth. An in planta Agrobacterium-mediated transformation protocol was used to introduce constructs into Arabidopsis (Bechtold et al., 1993; Clough and Bent, 1998). Selection of kanamycin- or hygromycin-resistant seedlings was performed on aseptic solid media containing 0.5 × MS salts (Murashige and Skoog, 1962; Sigma), 2% sucrose, and 1% purified agar (Sigma).

The *se fas1-1* double mutants were identified in the second generation after backcrossing *se* × *fas1-1* F_2 individuals with a Fas phenotype to *se*. Roughly one-quarter of the progeny from selfed Se backcross progeny displayed the described double mutant phenotype. The *se fas1-11* double mutants were identified among the F_2 progeny from a cross between se and *fas1-11.* Differences between the Columbia (Col-1) and Enkeim (En) ecotype backgrounds of the parental strains may have contributed to the broad range of observed phenotypes; however, very similar ranges of double mutant severities were seen in both the *se* × *fas1-1 SE*/*se* F_2 (3:1 Col-1:En) and the original *se* × *fas1-1* F_2 (1:1 Col-1:En), suggesting that other factors also contributed to the variability (data not shown).

Leaf outlines were traced using Deneba Canvas (Miami, FL) after the series of rosette leaves were scanned using a flatbed scanner. Scanning electron microscopy was performed as previously described (Pickett et al., 1996; Yu et al., 2000).

Molecular Biology Techniques

Plant genomic DNA was prepared in one of two ways. Large-scale preparations were isolated from lyophilized material by CTAB precipitation (Reiter et al., 1992). A scaled-down version of a protocol by Dean et al. (1992) was used for mini-preparations suitable for polymerase chain reaction (PCR) and DNA gel blot analyses and is described briefly. One or two leaves (~5 cm^2 total leaf area) were transferred to microcentrifuge tubes, frozen in liquid nitrogen, spun briefly in a microcentrifuge, and re-frozen. Using a polypropylene mini-pestle attached to a drill, the tissue was ground until it started to thaw. After adding 500 μL of extraction buffer (140 mM sorbitol, 220 mM Tris, pH 8, 22 mM EDTA, pH 8, 0.8 M NaCl, 1% sarkosyl, and 0.8% CTAB), the contents were mixed with the pestle. Samples were incubated at 60 to 65°C for 20 to 40 min with occasional mixing. Cooled samples were extracted with chloroform and ethanol precipitated. For PCR analysis, the pellet was washed with 70% ethanol, dried, and resuspended in 50 μL of TE (10 mM Tris and 0.5 mM EDTA, pH 8). For DNA gel blot analysis, the samples were resuspended in 100 μL of 300 mM NaCl and further extracted at least once with 1:1 phenol:chloroform then chloroform, precipitated, washed, dried, and resuspended in 20 μL of TE; the yield was determined using a DyNA Quant 200 fluorometer (Amersham Pharmacia Biotech).

To facilitate higher throughput PCR mapping, loading dyes and sucrose were included in the reaction mixtures (Hoppe et al., 1992). PCR reactions contained 50 mM KCl, 10 Tris-HCl, pH 8.3, 1 mM $MgCl_2$, 0.1 g/L BSA, 12% sucrose, 0.1% Triton X-100, 0.2 mM cresol red, 0.3% yellow food coloring (McCormick and Co., Inc., Hunt Valley, MD), 125 μM each dNTP, 250 nM each primer, and 0.1 U/μL Taq polymerase.

The non-radioactive Genius System (Boehringer Mannheim, Mannheim, Germany) was used—essentially as prescribed—for DNA gel blot analysis and for screening bacterial artificial chromosome (BAC) and phage libraries. Between 0.3 and 2 μg of restricted Arabidopsis genomic DNA was fractionated and blotted to nylon membranes for DNA gel blot analysis. Probe detection using alkaline phosphatase– and horseradish peroxidase–conjugated anti-digoxigenin antibodies was performed essentially as described by the manufacturer except that casein (U.S. Biochemical) was substituted for Boehringer Blocking powder and an extra post-antibody binding wash was added. CDP-Star was used for alkaline phosphatase detection, and luminol-based chemiluminescence was used for horseradish peroxidase detection.

Mapping the *SE* Locus

SE was initially mapped using a *se* (Col-1 ecotype) × Ws F_2 population, the *GPA1* and *PHYB* CAPS markers (Konieczny and Ausubel, 1993; Boerjan et al., 1995), and the nga168 and *AthGPA1* SSLP markers (Bell and Ecker, 1994). The locus was finely mapped using mapping lines with meiotic recombination near the *SE* locus derived from three different crosses: *se* × *phyB-10* (Ws ecotype), *se* × Tn28 (Landsberg *erecta* [L*er*] ecotype), and *se* × *alb3-1* (L*er* ecotype). Lines with breakpoints above of *SE* were identified as kanamycin-resistant (*phyB-10*/*PHYB*) or hygromycin-resistant (Tn28/+) *se*/*se* plants. Lines with breakpoints between *SE* and *ALB3* were identified as hygromycin-resistant (*alb3-1*/*ALB3*) *se*/*se* plants. Finally, lines with breakpoints between *ER* and *ALB3* were identified as non-albino *er*/*er* plants. These mapping lines were genotyped using the B68 restriction fragment length polymorphism (RFLP) marker (Ellen Wisman, Max-Planck-Institut, Cologne, Germany), *HY1* CAPS marker (Muramoto et al., 1999), nga1126 SSLP marker (http://thale.salk.edu/), and RFLP markers derived from BACs isolated during contig assembly (below).

Isolating the SE Locus

To minimize wear on individual BAC library filters, each of the 11 plates was prescreened by DNA gel blot analysis. Each of the first 11 plates of the TAMU BAC library (Choi et al., 1995) was stamped onto solid media and grown overnight, and the pooled colonies from each plate were collected for DNA preparation. HindIII-restricted plate-pool DNA (3 μg) were fractionated and blotted. Because the BACs were constructed using HindIII-restricted genomic DNA (Choi et al., 1995), diagnostically sized fragments were detected in positive plate pools, thus reducing the chances of false positives. Individual library

plates were then stamped onto nylon membranes, placed on solid media, and grown overnight, and the filters were prepared for hybridization (Sambrook et al., 1989). After identification, positive BACs were compared by HindIII restriction and DNA gel blot analysis. Digoxigenin-labeled BAC end probes were generated directly from the EcoRV-digested BACs using T7 RNA polymerase or by labeling subcloned end fragments. The BAC end subclones were isolated by end rescuing: religation after BamHI or SphI digestion (Sp6 ends) or after BstBI or BspDI digestion (both ends). In the latter case, the T7 ends were usually isolated by subcloning the appropriate BstBI-HindIII or HindIII fragment.

The BAC T9H20 was partially digested with HindIII and size-fractionated using low-melting-point agarose. Two size ranges (12 to 23 kb and 23 to 50 kb) were purified using β-agarase (New England Biolabs, Beverly, MA) and phenol:chloroform extraction (necessary to remove residual agarose). Both size-ranges were ligated into HindIII-digested and shrimp alkaline phosphatase–treated pOCA28 plant transformation vector, a derivative of pOCA18 obtained from Neil Olszewski (University of Minnesota, St. Paul; Olszewski et al., 1988). Ligation reactions were used in transforming ultra-competent *Escherichia coli* DH5αF′ cells (Inoue et al., 1990; Tang et al., 1994). DNA from 105 individual cosmids was prepared, digested with HindIII, run on a 1% agarose gel, and blotted to duplicate filters. The relative position of each cosmid was determined by comparing the restriction patterns and the hybridization patterns of several probes. Overlapping subclones were selected and transformed individually into *se* mutant plants. After selection on kanamycin-containing solid media, the phenotypes were noted. All transformants had a *se*-like phenotype except for those transformed with four overlapping subclones, which rescued the mutant phenotypes. The region of overlap between these cosmids was sequenced from cosmids directly or after subcloning. The region containing the *SE* gene was PCR-amplified from *se* mutant DNA, and pooled products from 10 independent reactions were purified and sequenced. Prior to publication, the region containing the *SE* gene was also sequenced by the Arabidopsis Genome Initiative (Lin et al., 1999; GenBank accession number AC005623). The determined genomic sequences were identical, although our *SE* cDNA sequence differed from the predicted At2g27100 mRNA sequence at the position of the splice-site acceptor site of the sixth intron.

cDNA Isolation

Expressed sequence tags (ESTs) corresponding to the *SE* gene (accession numbers T42213 and AA585883) and from a closely related gene from sugarcane (accession numbers AA080638 and AA080660) were obtained from ABRC and from D. Carson (South African Sugar Association Experiment Station, Mount Edgecombe, South Africa), respectively. These cDNAs were labeled and used as probes for screening λZAPII-based cDNA libraries derived from either Arabidopsis hypocotyls (Kieber et al., 1993) or maize leaves (Fisk et al., 1999) provided by ABRC and Alice Barkan (University of Oregon, Eugene), respectively. Ten positive Arabidopsis cDNA clones and seven maize cDNA clones were excised according to the manual provided by Stratagene (La Jolla, CA) and compared on agarose gels after XhoI-XbaI double digestion. The longest Arabidopsis cDNA was sequenced, and the 5′ end of each maize cDNA was sequenced initially. Two classes of maize clone sequences emerged after sequence comparisons, and the longest representative from each locus was used to finish sequencing. Simultaneously, the sugarcane cDNA was also sequenced. To indicate their paralogous nature, the names ZmSE1A and ZmSE1B were used for the maize loci. The GenBank accession numbers for the cDNA sequences are AF311221 through AF311224.

Protein Sequence Alignments

The GenBank accession numbers for the maize EST sequences used in Figure 5A are AI987373 and AW056145 for ZmSE2A; and AW330612 for ZmSE2B. Amino acid sequences were extracted from consensus EST, and a frameshift was introduced to the ZmSE2B sequence to preserve the open reading frame. The GenBank accession numbers (and references) for the *Schizosaccharomyces pombe*, Drosophila, and hamster Asr2 protein sequences are CAA22180 (*S. pombe* Sequencing Group at the Sanger Centre), AAF57281 (Adams et al., 2000), and AAA83777 (Rossman and Wang, 1999), respectively. The *Caenorhabditis elegans* protein sequence was deduced after manually splicing the genomic sequence (AC006627; Genome Sequencing Center, Washington University School of Medicine) on the basis of EST sequences, and the human protein sequence was deduced after manually splicing the chromosome 7 working draft sequences (NT007969; International Human Genome Sequencing Consortium, 2001) on the basis of the DKFZp564H2023 cDNA sequence (AL096723).

Protein sequences were initially aligned using the PILEUP program (Genetics Computer Group, Madison, WI) and then manually adjusted. Figures were generated using MacBoxshade (Michael D. Baron, Institute for Animal Health, UK) and modified using Deneba Canvas (Miami, FL).

In Situ Detection of the *SE* mRNA

The tissue preparation and detection protocols followed for the in situ detection of *SE* mRNA were based on those described previously (Long and Barton, 1998; http://www.wisc.edu/genetics/CATG/barton/index.html) except that a 3-hr prehybridization step replaced the dehydration and drying step (Larkin et al., 1993). Digoxigenin-labeled riboprobes were synthesized from each strand of the full-length *SE* cDNA insert by in vitro transcription by the T7 (anti-sense strand) and T3 (sense strand) RNA polymerases. Probe yield was determined by spot test (relative to a labeled DNA standard), and the probe was diluted to 50 ng/mL for hybridization.

Misexpressing the *SE* Gene

To replace the β-glucuronidase coding sequence of the pBI121 plant expression vector (Clontech Co., Palo Alto, CA) with the *SE* coding sequence, a BamHI restriction site was added 5′ from the *SE* initiation codon. A primer was designed that replaced nucleotides aacgaaATGgcc of the cDNA (initiation codon in capital letters) to ggatccATGgcc, creating a BamHI (as well as a NcoI) site. A PCR fragment containing this mutated sequence was cloned into a pBluescript II vector (Stratagene, La Jolla, CA) and sequenced. The full-length coding sequence was reconstituted using a BsaBI site 11 nucleotides 3′ from the initiation codon. The resulting cDNA was inserted into the pBI121 vector for introduction into plants. Transformed plants were identified by selection on kanamycin-containing media.

Reverse Transcriptase–PCR

Mini-preparations of total leaf RNA were performed as previously described (Carpenter and Simon, 1998). M-MLV reverse transcriptase (RT) (Promega, Madison, WI) and a poly (dT) primer were used to generate the cDNA templates for PCR. PCR conditions were the same as described above except that only 10 cycles were performed prior to gel fractionation. To control for differences in loading, two ubiquitously expressed genes were detected using the same cDNA preparations: the *ROC1* cyclophilin gene (Lippuner et al., 1994) and the Arabidopsis ortholog of the tobacco *β-ATPase* gene (Boutry and Chua, 1985; Kelly et al., 1990). The PCR primers used were the following: *SE*, ctgttgtctccggcctttag and ctctagccctgtcttgtctac; *ROC1*, gatctacgggagcaagttcg and ttctcgatggcctttaccac; and *β-ATPase*, gtgcccgtaagatcc-agaga and tcttctctgcctttgcaacc.

ACKNOWLEDGMENTS

We thank Kris Soebroto for assistance in mapping, Yanling Wang of the Institute of Molecular Biology Sequencing Facility for sequencing, and Karen Hicks, Steve Clark, and Sang Ho Jeong for helpful comments on the manuscript. We thank Hidetaka Kaya and Takashi Araki for sharing unpublished results and the Arabidopsis Biological Resource Center, Eva Sundberg and George Coupland, Deborah Lee Carson, and Alice Barkan for supplying materials. We are indebted to George Rédei for sharing his mutant collection. This research was supported by National Science Foundation Grant MCB-9808208 and the U.S.-Israel Binational Agricultural Research and Development (BARD) Agency Grant US-2964-97. M.J.P. was supported by predoctoral training grants from the National Science Foundation (DBI-9413223) and National Institutes of Health (GM07413).

Received March 7, 2001; accepted April 4, 2001.

REFERENCES

Adams, C.R., and Kamakaka, R.T. (1999). Chromatin assembly: Biochemical identities and genetic redundancy. Curr. Opin. Genet. Dev. **9,** 185–190.

Adams, M.D., et al. (2000). The genome sequence of *Drosophila melanogaster*. Science **287,** 2185–2195.

Baskin, T.I., Cork, A., Williamson, R.W., and Gorst, J.R. (1995). *STUNTED PLANT 1*, a gene required for expansion in rapidly elongating but not in dividing cells and mediating root growth responses to applied cytokinin. Plant Physiol. **107,** 233–243.

Bechtold, N., Ellis, J., and Pelletier, G. (1993). In planta *Agrobacterium* gene transfer by infiltration of adult *Arabidopsis thaliana* plants. C. R. Acad. Sci. Paris Life Sci. **316,** 1195–1197.

Bell, C.J., and Ecker, J.R. (1994). Assignment of 30 microsatellite loci to the linkage map of *Arabidopsis*. Genomics **19,** 137–144.

Berg, J.M., and Shi, Y. (1996). The galvanization of biology: A growing appreciation for the roles of zinc. Science **271,** 1081–1085.

Berná, G., Robles, P., and Micol, J.L. (1999). A mutational analysis of leaf morphogenesis in *Arabidopsis thaliana*. Genetics **152,** 729–742.

Boerjan, W., Cervera, M.T., Delarue, M., Beeckman, T., Dewitte, W., Bellini, C., Caboche, M., Van Onckelen, H., Van Montagu, M., and Inze, D. (1995). *superroot*, a recessive mutation in *Arabidopsis*, confers auxin overproduction. Plant Cell **7,** 1405–1419.

Bohmert, K., Camus, I., Bellini, C., Bouchez, D., Caboche, M., and Benning, C. (1998). *AGO1* defines a novel locus of *Arabidopsis* controlling leaf development. EMBO J. **17,** 170–180.

Boutry, M., and Chua, N.-H. (1985). A nuclear gene encoding the beta subunit of the mitochondrial ATP synthase in *Nicotiana plumbaginifolia*. EMBO J. **4,** 2159–2165.

Byrne, M.E., Barley, R., Curtis, M., Arroyo, J.M., Dunham, M., Hudson, A., and Martienssen, R.A. (2000). *Asymmetric leaves1* mediates leaf patterning and stem cell function in *Arabidopsis*. Nature **408,** 967–971.

Carpenter, C.D., and Simon, A.E. (1998). Preparation of RNA. In Arabidopsis Protocols, J.M. Martínez-Zapater and J. Salinas, eds (Totowa, NJ: Humana Press, Inc.), pp. 85–89.

Champagne, M.M. (1998). Genetic Regulation of Shoot Development in *Arabidopsis thaliana*. Ph.D. Dissertation (Eugene, OR: University of Oregon).

Chaudhury, A.M., Ming, L., Miller, C., Craig, S., Dennis, E.S., and Peacock, W.J. (1997). Fertilization-independent seed development in *Arabidopsis thaliana*. Proc. Natl. Acad. Sci. USA **94,** 4223–4228.

Chien, J.C., and Sussex, I.M. (1996). Differential regulation of trichome formation on the adaxial and abaxial leaf surfaces by gibberellins and photoperiod in *Arabidopsis thaliana* (L.) Heynh. Plant Physiol. **111,** 1321–1328.

Choi, S., Creelman, R.A., Mullet, J.E., and Wing, R.A. (1995). Construction and characterization of a bacterial artificial chromosome library of *Arabidopsis thaliana*. Plant Mol. Biol. Rep. **13,** 124–128.

Clarke, J.H., Tack, D., Findlay, K., Van Montagu, M., and Van Lijsebettens, M. (1999). The *SERRATE* locus controls the formation of the early juvenile leaves and phase length in *Arabidopsis*. Plant J. **20,** 493–501.

Clough, S.J., and Bent, A.F. (1998). Floral dip: A simplified method for *Agrobacterium*-mediated transformation of *Arabidopsis thaliana*. Plant J. **16,** 735–744.

Cockcroft, C.E., den Boer, B.G., Healy, J.M., and Murray, J.A. (2000). Cyclin D control of growth rate in plants. Nature **405,** 575–579.

Dean, C., Sjodin, C., Page, T., Jones, J., and Lister, C. (1992). Behavior of the maize transposable element *Ac* in *Arabidopsis thaliana*. Plant J. **1,** 69–81.

Elliott, R.C., Betzner, A.S., Huttner, E., Oakes, M.P., Tucker, W.Q., Gerentes, D., Perez, P., and Smyth, D.R. (1996). *AINTEGUMENTA*, an *APETALA2*-like gene of Arabidopsis with pleiotropic roles in ovule development and floral organ growth. Plant Cell **8,** 155–168.

Emmler, K., and Schäfer, E. (1997). Maternal effect on embryogenesis in tobacco overexpressing rice phytochrome A. Bot. Acta **110,** 1–8.

Enomoto, S., and Berman, J. (1998). Chromatin assembly factor I contributes to the maintenance, but not the re-establishment, of silencing at the yeast silent mating loci. Genes Dev. **12,** 219–232.

Enomoto, S., McCune-Zierath, P.D., Gerami-Nejad, M., Sanders, M.A., and Berman, J. (1997). RLF2, a subunit of yeast chromatin

assembly factor-I, is required for telomeric chromatin function in vivo. Genes Dev. **11,** 358–370.

Farkas, G., Gausz, J., Galloni, M., Reuter, G., Gyurkovics, H., and Karch, F. (1994). The *Trithorax-like* gene encodes the *Drosophila* GAGA factor. Nature **371,** 806–808.

Fisk, D.G., Walker, M.B., and Barkan, A. (1999). Molecular cloning of the maize gene *crp1* reveals similarity between regulators of mitochondrial and chloroplast gene expression. EMBO J. **18,** 2621–2630.

Goodrich, J., Puangsomlee, P., Martin, M., Long, D., Meyerowitz, E.M., and Coupland, G. (1997). A polycomb-group gene regulates homeotic gene expression in *Arabidopsis*. Nature **386,** 44–51.

Groot, E.P., and Meicenheimer, R.D. (2000a). Comparison of leaf plastochron index and allometric analyses of tooth development in *Arabidopsis thaliana*. J. Plant Growth Regul. **19,** 77–89.

Groot, E.P., and Meicenheimer, R.D. (2000b). Short-day-grown *Arabidopsis thaliana* satisfies the assumptions of the plastochron index as a time variable in development. Int. J. Plant Sci. **161,** 749–756.

Grossniklaus, U., Vielle-Calzada, J.P., Hoeppner, M.A., and Gagliano, W.B. (1998). Maternal control of embryogenesis by *MEDEA*, a polycomb group gene in *Arabidopsis*. Science **280,** 446–450.

Hempel, F.D., and Feldman, L.J. (1994). Bi-directional inflorescence development in *Arabidopsis thaliana*: Acropetal initiation of flowers and basipetal initiation of paraclades. Planta **192,** 276–286.

Hoppe, B.L., Conti-Tronconi, B.M., and Horton, R.M. (1992). Gel-loading dyes compatible with PCR. Biotechniques **12,** 679–680.

Inoue, H., Nojima, H., and Okayama, H. (1990). High efficiency transformation of *Escherichia coli* with plasmids. Gene **96,** 23–28.

International Human Genome Sequencing Consortium. (2001). Initial sequencing and analysis of the human genome. Nature **409,** 860–921.

Kaufman, P.D., Kobayashi, R., and Stillman, B. (1997). Ultraviolet radiation sensitivity and reduction of telomeric silencing in *Saccharomyces cerevisiae* cells lacking chromatin assembly factor-I. Genes Dev. **11,** 345–357.

Kaya, H., Shibahara, K., Taoka, K., Iwabuchi, M., Stillman, B., and Araki, T. (2001). *FASCIATA* genes for chromatin assembly factor-1 in *Arabidopsis* maintain the cellular organization of apical meristems. Cell **104,** 131–142.

Kelly, A.J., Zagotta, M.T., White, R.A., Chang, C., and Meeks-Wagner, D.R. (1990). Identification of genes expressed in the tobacco shoot apex during the floral transition. Plant Cell **2,** 963–972.

Kerstetter, R.A., and Poethig, R.S. (1998). The specification of leaf identity during shoot development. Annu. Rev. Cell Dev. Biol. **14,** 373–398.

Kieber, J.J., Rothenberg, M., Roman, G., Feldmann, K.A., and Ecker, J.R. (1993). *CTR1*, a negative regulator of the ethylene response pathway in Arabidopsis, encodes a member of the raf family of protein kinases. Cell **72,** 427–441.

Kinoshita, T., Yadegari, R., Harada, J.J., Goldberg, R.B., and Fischer, R.L. (1999). Imprinting of the *MEDEA* polycomb gene in the Arabidopsis endosperm. Plant Cell **11,** 1945–1952.

Kiyosue, T., Ohad, N., Yadegari, R., Hannon, M., Dinneny, J., Wells, D., Katz, A., Margossian, L., Harada, J.J., Goldberg, R.B., and Fischer, R.L. (1999). Control of fertilization-independent endosperm development by the *MEDEA* polycomb gene in *Arabidopsis*. Proc. Natl. Acad. Sci. USA **96,** 4186–4191.

Klucher, K.M., Chow, H., Reiser, L., and Fischer, R.L. (1996). The *AINTEGUMENTA* gene of Arabidopsis required for ovule and female gametophyte development is related to the floral homeotic gene *APETALA2*. Plant Cell **8,** 137–153.

Klug, A., and Schwabe, J.W. (1995). Protein motifs 5. Zinc fingers. FASEB J. **9,** 597–604.

Konieczny, A., and Ausubel, F.M. (1993). A procedure for mapping *Arabidopsis* mutations using co-dominant ecotype-specific PCR-based markers. Plant J. **4,** 403–410.

Larkin, J.C., Oppenheimer, D.G., Pollock, S., and Marks, M.D. (1993). The Arabidopsis *GLABROUS1* gene requires downstream sequences for function. Plant Cell **5,** 1739–1748.

Larkin, J.C., Oppenheimer, D.G., Lloyd, A.M., Paparozzi, E.T., and Marks, M.D. (1994). Roles of the *GLABROUS1* and *TRANSPARENT TESTA GLABRA* genes in Arabidopsis trichome development. Plant Cell **6,** 1065–1076.

Laufs, P., Dockx, J., Kronenberger, J., and Traas, J. (1998). *MGOUN1* and *MGOUN2*: Two genes required for primordium initiation at the shoot apical and floral meristems in *Arabidopsis thaliana*. Development **125,** 1253–1260.

Leyser, H.M.O., and Furner, I.J. (1992). Characterisation of three shoot apical meristem mutants of *Arabidopsis thaliana*. Development **116,** 397–403.

Lin, X., et al. (1999). Sequence and analysis of chromosome 2 of the plant *Arabidopsis thaliana*. Nature **402,** 761–768.

Lippuner, V., Chou, I.T., Scott, S.V., Ettinger, W.F., Theg, S.M., and Gasser, C.S. (1994). Cloning and characterization of chloroplast and cytosolic forms of cyclophilin from *Arabidopsis thaliana*. J. Biol. Chem. **269,** 7863–7868.

Liu, Z., and Meyerowitz, E.M. (1995). *LEUNIG* regulates *AGAMOUS* expression in *Arabidopsis* flowers. Development **121,** 975–991.

Long, D., Martin, M., Sundberg, E., Swinburne, J., Puangsomlee, P., and Coupland, G. (1993). The maize transposable element system *Ac*/*Ds* as a mutagen in *Arabidopsis*: Identification of an *albino* mutation induced by *Ds* insertion. Proc. Natl. Acad. Sci. USA **90,** 10370–10374.

Long, J.A., and Barton, M.K. (1998). The development of apical embryonic pattern in *Arabidopsis*. Development **125,** 3027–3035.

Luo, M., Bilodeau, P., Koltunow, A., Dennis, E.S., Peacock, W.J., and Chaudhury, A.M. (1999). Genes controlling fertilization-independent seed development in *Arabidopsis thaliana*. Proc. Natl. Acad. Sci. USA **96,** 296–301.

Lynn, K., Fernandez, A., Aida, M., Sedbrook, J., Tasaka, M., Masson, P., and Barton, M.K. (1999). The *PINHEAD*/*ZWILLE* gene acts pleiotropically in *Arabidopsis* development and has overlapping functions with the *ARGONAUTE1* gene. Development **126,** 469–481.

Martínez-Zapater, J.M., Jarillo, J.A., Cruz-Alverez, M., Roldán, M., and Salinas, J. (1995). *Arabidopsis* late-flowering *fve* mutants are affected in both vegetative and reproductive development. Plant J. **7,** 543–551.

Matzke, A.J., and Matzke, M.A. (1998). Position effects and epigenetic silencing of plant transgenes. Curr. Opin. Plant Biol. **1,** 142–148.

Muramoto, T., Kohchi, T., Yokota, A., Hwang, I., and Goodman, H.M. (1999). The Arabidopsis photomorphogenic mutant *hy1* is deficient in phytochrome chromophore biosynthesis as a result of a mutation in a plastid heme oxygenase. Plant Cell **11,** 335–348.

Murashige, T., and Skoog, F. (1962). A revised medium for rapid growth and bioassays with tobacco tissue culture. Physiol. Plant **15,** 473–497.

Odell, J.T., Nagy, F., and Chua, N.H. (1985). Identification of DNA sequences required for activity of the cauliflower mosaic virus 35S promoter. Nature **313,** 810–812.

Ohad, N., Yadegari, R., Margossian, L., Hannon, M., Michaeli, D., Harada, J.J., Goldberg, R.B., and Fischer, R.L. (1999). Mutations in *FIE*, a WD polycomb group gene, allow endosperm development without fertilization. Plant Cell **11,** 407–416.

Olszewski, N.E., Martin, F.B., and Ausubel, F.M. (1988). Specialized binary vector for plant transformation: Expression of the *Arabidopsis thaliana AHAS* gene in *Nicotiana tabacum*. Nucleic Acids Res. **16,** 10765–10782.

Ori, N., Eshed, Y., Chuck, G., Bowman, J.L., and Hake, S. (2000). Mechanisms that control *knox* gene expression in the *Arabidopsis* shoot. Development **127,** 5523–5532.

Pedone, P.V., Ghirlando, R., Clore, G.M., Gronenborn, A.M., Felsenfeld, G., and Omichinski, J.G. (1996). The single Cys2-His2 zinc finger domain of the GAGA protein flanked by basic residues is sufficient for high-affinity specific DNA binding. Proc. Natl. Acad. Sci. USA **93,** 2822–2826.

Pickett, F.B., Champagne, M.M., and Meeks-Wagner, D.R. (1996). Temperature-sensitive mutations that arrest *Arabidopsis* shoot development. Development **122,** 3799–3807.

Pillus, L., and Rine, J. (1989). Epigenetic inheritance of transcriptional states in *S. cerevisiae*. Cell **59,** 637–647.

Ptashne, M. (1992). A Genetic Switch: Phage λ and Higher Organisms (Cambridge, MA: Cell Press, Blackwell Scientific Publications).

Ray, S., Golden, T., and Ray, A. (1996). Maternal effects of the *short integument* mutation on embryo development in *Arabidopsis*. Dev. Biol. **180,** 365–369.

Rédei, G.P., and Hirono, Y. (1964). Linkage studies. Arabidopsis Info. Serv. **1,** 9–10.

Reiser, L., Sánchez-Baracaldo, P., and Hake, S. (2000). Knots in the family tree: Evolutionary relationships and functions of *knox* homeobox genes. Plant Mol. Biol. **42,** 151–166.

Reiter, R.S., Young, R.M., and Scolnik, P.A. (1992). Genetic linkage of the *Arabidopsis* genome: Methods for mapping with recombinant inbreds and random amplified polymorphic DNAs (RAPDs). In Methods in Arabidopsis Research, C. Koncz, N.-H. Chua, and J. Schell, eds (River Edge, NJ: World Scientific Press, Inc.), pp. 170–190.

Roe, J.L., Rivin, C.J., Sessions, R.A., Feldmann, K.A., and Zambryski, P.C. (1993). The *Tousled* gene in *A. thaliana* encodes a protein kinase homolog that is required for leaf and flower development. Cell **75,** 939–950.

Rossman, T.G., and Wang, Z. (1999). Expression cloning for arsenite-resistance resulted in isolation of tumor-suppressor *fau* cDNA: Possible involvement of the ubiquitin system in arsenic carcinogenesis. Carcinogenesis **20,** 311–316.

Sambrook, J., Fritsh, E.F., and Maniatis, T. (1989). Molecular Cloning: A Laboratory Manual, 2nd ed. (Cold Spring Harbor, NY: Cold Spring Harbor Press).

Serrano-Cartagena, J., Robles, P., Ponce, M.R., and Micol, J.L. (1999). Genetic analysis of leaf form mutants from the *Arabidopsis* Information Service collection. Mol. Gen. Genet. **261,** 725–739.

Smith, S., and Stillman, B. (1989). Purification and characterization of CAF-I, a human cell factor required for chromatin assembly during DNA replication *in vitro*. Cell **58,** 15–25.

Smyth, D.R., Bowman, J.L., and Meyerowitz, E.M. (1990). Early flower development in *Arabidopsis*. Plant Cell **2,** 755–767.

Steeves, T.A., and Sussex, I.M. (1989). Patterns in Plant Development, 2nd ed. (Cambridge, UK: Cambridge University Press).

Tang, X., Nakata, Y., Li, H.-O., Zhang, M., Gao, H., Fujita, A., Sakatsume, O., Ohta, T., and Yokayama, K. (1994). The optimization of preparations of competent cells for transformation of *E. coli*. Nucleic Acids Res. **22,** 2857–2858.

Telfer, A., Bollman, K.M., and Poethig, R.S. (1997). Phase change and the regulation of trichome distribution in *Arabidopsis thaliana*. Development **124,** 645–654.

Timmermans, M.C., Hudson, A., Becraft, P.W., and Nelson, T. (1999). ROUGH SHEATH2: A myb protein that represses *knox* homeobox genes in maize lateral organ primordia. Science **284,** 151–153.

Tsiantis, M., Schneeberger, R., Golz, J.F., Freeling, M., and Langdale, J.A. (1999). The maize *rough sheath2* gene and leaf development programs in monocot and dicot plants. Science **284,** 154–156.

van der Veen, J.H., and Wirtz, P. (1968). EMS-induced genic male sterility in *Arabidopsis thaliana*: A model selection experiment. Euphytica **17,** 371–377.

Vernon, D.M., and Meinke, D.W. (1995). Late *embryo-defective* Mutants of *Arabidopsis*. Dev. Genet. **16,** 311–320.

Vielle-Calzada, J.P., Thomas, J., Spillane, C., Coluccio, A., Hoeppner, M.A., and Grossniklaus, U. (1999). Maintenance of genomic imprinting at the *Arabidopsis medea* locus requires zygotic *DDM1* activity. Genes Dev. **13,** 2971–2982.

Waites, R., and Hudson, A. (1995). *phantastica*: A gene required for dorsoventrality of leaves in Antirrhinum majus. Development **121,** 2143–2154.

Waites, R., Selvadurai, H.R., Oliver, I.R., and Hudson, A. (1998). The *PHANTASTICA* gene encodes a MYB transcription factor involved in growth and dorsoventrality of lateral organs in *Antirrhinum*. Cell **93,** 779–789.

Wilkins, R.C., and Lis, J.T. (1997). Dynamics of potentiation and activation: GAGA factor and its role in heat shock gene regulation. Nucleic Acids Res. **25,** 3963–3968.

Yu, L.P., Simon, E.J., Trotochaud, A.E., and Clark, S.E. (2000). *POLTERGEIST* functions to regulate meristem development downstream of the *CLAVATA* loci. Development **127,** 1661–1670.